Universities of Leeds, Sheffield and York
http://eprints.whiterose.ac.uk/

Published paper

Measurement of deformation gradients in hot rolling of AA3004

C. Boldetti, C. Pinna, I.C. Howard, G. Gutierrez

IMMPETUS, Department of Mechanical Engineering, The University of Sheffield
Mappin Street, Sheffield S1 3JD, Sheffield, UK

Abstract

In this paper we describe an experimental technique developed to measure the deformation gradients and temperature in a single hot rolling pass of an AA3004 sample that was fitted with an insert. The insert had been previously hand engraved with a *1x1 mm* grid pitch and the analysis of the data digitally captured from the image of the deformed grid enabled the calculation of the components of the deformation gradient tensor. Four steel pins prevented relative motion between the insert and the rest of the sample. No detachment was observed between insert and sample after rolling. The temperature was measured during rolling using two embedded thermocouples, one close to the surface and the other in the centreline. The commercial finite element code ABAQUS was used to create a three-dimensional model of the rolling process. The recorded temperature was compared to the numerical values evaluated after tuning the heat transfer coefficient. The shape of the grid after rolling was checked against the deformed mesh using different friction coefficients in order to obtain the optimum match. The unusually large length of the insert enabled the rolling process to be stopped halfway so that a picture of the roll-gap area could be obtained. This provided a partially deformed grid that represented the transient state during rolling. The experimentally determined deformation gradient in this area as well as in the steady state area agreed well with the finite-element predictions.

Keywords

Hot rolling, grid, deformation gradient, aluminium alloy, finite element modelling.

Introduction

   Accurate prediction of the development and distribution of the deformation of hot worked metals like aluminium alloys is of considerable importance to the metal industry. Amongst other things, this is due to the fact that plastic deformation in the early stages of aluminium rolling is significantly heterogeneous. This usually results in considerable microstructural differences through the thickness of the rolled material. This heterogeneity of deformation also leads to the development of different deformation textures between the surface and the centre of the slab. [1] Contemporary models for the prediction of such deformation texture require, as input, values for the components of the deformation gradient tensor [2], which not only include the strain but also the rotation of a material element as it moves through the roll gap. The deformation gradient tensor invariably comes from finite element (FE) models of the forming process under investigation. The output of such models is sensitive to variations in a large range of input variables and relationships, particularly, in metal forming, those associated with the details of load, friction and heat transfer across the contacting interfaces between the tools and work-piece.

   The issues discussed above provide a specific and direct technological need for independent validation of the techniques of obtaining deformation gradients from finite element models of forming processes. More generally, the patterns of deformation during metal rolling are fundamentally important to almost all consideration of what is happening to the material and its microstructure. As noted above, finite element (or other numerical) models are sensitive to the parameters controlling friction and heat transfer between tool and work-piece, and require experimental validation. There have been several attempts at this in the past, with varying degrees of success. Previous publications, few in number, showed different attempts to

validate the numerical models through temperature measurements and rolling loads.[3] [4] [5] The evaluation of the temperature is important to give an idea of the *heat transfer coefficient* and the microstructural changes but does not help define the deformation gradient, while the measurement of the rolling load is a general indication and does not account for the local values of the strain through the thickness of the slab.

Timothy *et al.* [5] used an engraved insert on a sample of a 5083 aluminium alloy and built a two-dimensional FE model with a rather coarse mesh for the stock whereas the roll was not meshed. More sophisticated FE models were attempted in the past [6] [7] [8], focusing on the modelling of friction, heat transfer coefficient and microstructural issues. However these finite element models are often validated by means of variables that do not consider the strain or the deformation gradients through the thickness. The temperature, the rolling load or the speed of the stock are measured and compared with the numerical data, giving a general idea of the reliability of the model but little insight into the accuracy of the strain values calculated through the thickness of the slab.

Wells *et al.* [9] worked on the same 5083 alloy and made use of a grid on the edge of the sample. Li *et al.* [10] used digital image correlation methods to measure the velocity field on the edge of the slab during cold rolling. However, a measurement of the deformation in the centre-plane of the specimen rather than on the edge is more significant since the deformation conditions at this location are closer to the plane strain conditions commonly assumed in rolling models of flat products. Even when an insert is used, with the gridded face laying on the centre-plane of the specimen, the work piece containing the insert has to be wide enough to ensure plane strain conditions on that plane. It is also important that the insert does not detach from the specimen, because in that case the deformed grid would not be representative of the deformation of a more standard specimen without insert. In steel samples the insert can be welded to the sample but some difficulties occur with aluminium due to the poor strength of the weld [11]: a mechanical solution has to be used to ensure continuous contact between insert and sample at high temperatures and high reduction ratios. In this work, steel pins were used to achieve continuity between insert and specimen and avoid detachment between them.
The embedded pin technique has also been used in many research projects [8][12] to measure the through-thickness deformation, but it presents some disadvantages, such as the detachment between pin and material and the limited area where the deformation can be observed.

The work described below was to measure in detail both the temperature and the deformation gradient in samples of a commercial aluminium alloy rolled in a laboratory mill under conditions that represented, as far as the constraints of the laboratory mill allowed, the last pass of breakdown rolling in an industrial process. A grid technique was used to measure the deformation gradient and the commercial finite-element code ABAQUS/Standard ver. 6.4, enhanced with user-developed subroutines, was employed to model the rolling process.

Experimental work

The experiments were performed on a 50-ton rolling mill with 68 *mm* diameter steel rollers and a furnace in close proximity. Four identical samples were machined (fig. 1). Two of them were completely rolled, giving similar results and one of them was only partially rolled by stopping the rollers. One sample could not be used as it was heavily bent after sticking to one of the rollers. Each specimen was 210 *mm* long, 60 *mm* wide and 20 *mm* thick. The large width of the sample ensured plane strain conditions on the centre-plane, where the gridded face of the insert is located. The samples were centrally slotted in order to embed the insert which had been previously engraved with a regular grid with a pitch of 1mm x 1mm. A height gauge equipped with a carbide tipped scriber was used to engrave the grid, whose depth, measured with a mechanical profilometer, was about 50 μm on average.

The insert chosen for the experiments was long enough to allow the rolling to stop halfway and study not only the state at output but also the roll-gap area and therefore the deformation gradients in the transition state. The back of the specimen (left-hand end of the specimen in fig.1) was machined in such a way as to make it easier for the operator to remove it from the furnace with tongs and quickly present it to the mill in order to avoid significant temperature drop due to air cooling. The front of the sample (right-hand end of the specimen in fig.1) was cut with an angle of about 20° to help the rolls drag the sample in the initial phase of the rolling.

Two type-K thermocouples with a diameter of 1.6 *mm* were fitted in two holes, one in the centreline, the other *3 mm* under the surface. The thermocouples were put in place and secured by punching the immediate surrounding of the holes on the side of the sample: this operation is important to avoid any loss of contact between the head of the thermocouple and the material during the high deformation due to rolling.

In order to avoid relative motion between sample and insert, the latter was secured against the sample by four through-width steel pins (fig. 1).
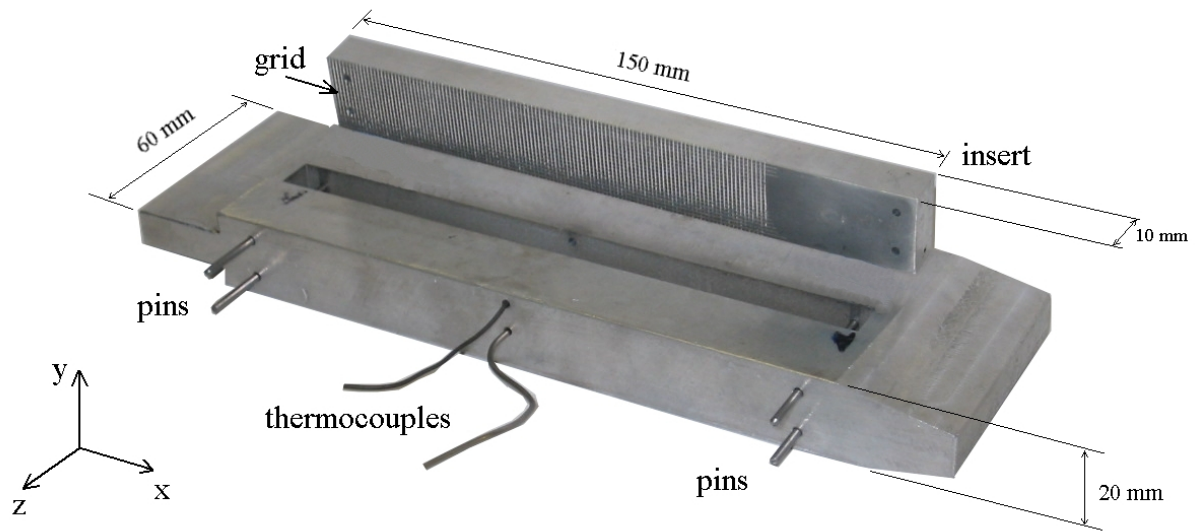
Figure 1 – Overview of the work-piece and insert. Two thermocouples were used to monitor the temperature and four steel pins ensured close contact between insert and work-piece during rolling. The insert was hand-engraved with a 1*mm* x 1*mm* grid pitch.

The aluminium alloy chosen for this work (table 1) is a commercial alloy mostly used for the body of beverage cans and storage tanks and it is produced through a complex rolling process.

AA3004 composition	Si	Fe	Cu	Mn	Mg	Zn
Weight %	0.3	0.7	0.25	1.0	0.8-1.3	0.25

Table 1 – Composition of 3004 aluminium alloy

The temperature was brought up to 400°C and the samples were left in the furnace for two hours in order to achieve a homogeneous temperature. The temperature was monitored through the thermocouples already in place in the specimen. The samples were rolled in a single 50% reduction pass at 11 revolutions per minute (rpm) and then quenched in water. No lubricant was used in these tests.

One of the samples was only partially rolled by stopping the rolls halfway through the rolling process: this left material "frozen-in" the nip of the mill, with the gridded insert providing a picture of the deformation of the material during its passage through the nip. This, coupled with the state of the gridded insert in the completely rolled specimens, provided a complete picture of the deformation during the rolling experiments.

After being rolled and quenched, the sample was opened up by carefully cutting longitudinally and the insert was extracted. After the tests, no gap was observed between the insert and the specimen (fig. 2), confirming the effectiveness of the pins in ensuring close contact under high deformation. No detachment was observed along the transverse direction. In addition, the face of the sample in contact with the grids was found to have grids in relief showing further evidence of close contact.

Moreover the specimen after rolling was relatively straight indicating a successful rolling procedure.

Figure 2 – Deformed specimen after rolling. The specimen is relatively straight and no detachment can be observed between insert and work-piece in both transverse and longitudinal direction.

Figure 3 shows a picture of the grid after rolling. The grid survived the test and the engraved lines can clearly be seen although the width of the lines is significant compared with the pitch.
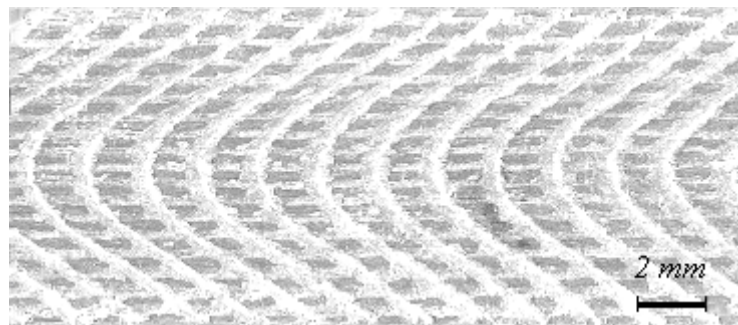
Figure 3 – Deformed grid after rolling. The width of the lines is significant compared to the pitch.

Deformation Gradient Tensor

The experiments showed that at a scale of the grid-pitch, a square in the undeformed state transforms into a trapezium after deformation. Hence the deformation gradient tensor, which contains information about both the deformation and the rotation of the element, appears to be a linear mapping between the initial and final states (fig. 4).
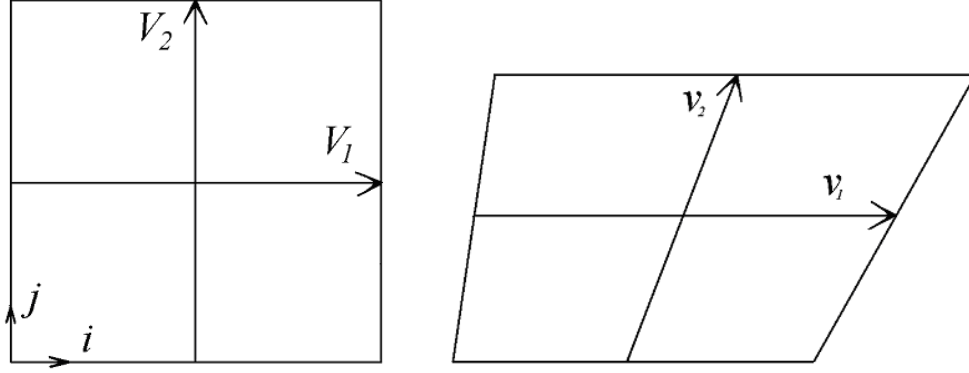
Figure 4 – Single square of the grid before deformation (left) and after deformation (right). The deformation gradient was calculated by comparing the two vectors V_1 and V_2 to the same vectors after deformation (v_1 and v_2) according to equation 3.

V_1 and V_2 (v_1 and v_2) in figure 4 are the two vectors that link the middle of the opposite sides of a given square, in the undeformed (deformed) configuration. They are defined as follows:

$$V_1 = Ai + Bj$$
$$V_2 = Ci + Dj ,$$
$$\qquad\qquad\qquad 1)$$

and the corresponding deformed vectors

$$v_1 = ai + bj$$
$$v_2 = ci + dj ,$$
$$\qquad\qquad\qquad 2)$$

The calculation of the deformation gradient tensor F was performed at the centroid of each element, using equation 3.

$$\begin{bmatrix} a & c \\ b & d \end{bmatrix} = F \cdot \begin{bmatrix} A & C \\ B & D \end{bmatrix} \qquad \Rightarrow \qquad F = \begin{bmatrix} a & c \\ b & d \end{bmatrix} \begin{bmatrix} A & C \\ B & D \end{bmatrix}^{-1} \qquad 3)$$

A MATLAB script was written to automate the coordinate extraction from a scanned image of the deformed grid. Because of the large size of the inserts used in this work, it proved convenient to digitise the picture with a computer scanner set to a resolution of 600 dpi (23.62 pixels/*mm*). Automatic recognition of the coordinates of the intersections did not seem possible given the width of the engraved grooves (up to 0.2 *mm*, which must be compared with the 1 *mm* grid pitch) and the difficulty of adjusting the picture brightness and contrast on the whole insert satisfactorily. As a result, manual plotting with the computer mouse was finally chosen as the method for coordinate extraction.

Confidence in the reliability of this technique depended first upon estimating its accuracy, since it was susceptible to random variations induced by the method of engraving and errors (which could be random or systematic) due to manual plotting. Accuracy in manual plotting

was first assessed by applying the script to a drawing of a perfect black square over a white background. The final deformation gradient tensor should, in theory, equal the identity tensor for an accurate method. The optimum contrast and the very thin lines led to a relative error that was less than 0.2%, this low value being obtained using a zoom function that helped increase the plotting accuracy. The assessment of plotting accuracy was then applied to a real engraved grid. The lower quality of the picture contrast together with the non-uniform width of the grooves made the plotting more difficult to perform. When clicking on grid intersections, the inaccuracy increases as the ratio of the groove width to the pitch size increases. Therefore the error had to be estimated for each component of the tensor F, using an engraved grid that featured pitches close to those of experimentally deformed grids. After this analysis, the statistical error was estimated from the standard deviation of the calculated values. The final error could be reduced by averaging (over sets of five grid elements) the calculations along a material streamline. This led to very acceptable statistical errors, as displayed in table 2.

	F_{xx}	F_{xy}	F_{yx}	F_{yy}
Experimental values	1.8	0.6	0.04	0.52
Absolute error	0.0056	0.0035	0.0032	0.0124
Relative error	0.3%	0.6%	8.0%	2.4%

Table 2 – Estimation of the error in the experimental measurements of the deformation gradient F, when averaged over five elements of the grid along the rolling direction.

Finite Element Model

The numerical simulation was developed using an implicit non-linear code, ABAQUS/Standard ver. 6.4, which employs a coupled thermal-stress analysis and a modified Coulomb friction model to represent the contact conditions. The roll was also meshed in order to better simulate the heat exchange during the process. However, a sensitivity analysis done by modelling a number of different geometries for the roll confirmed that, at the rolling speed used for this simulation (11 rpm), only the first *5 mm* of the thickness of the roll was needed to model the thermal gradient in the roll. Due to symmetry, only half of the slab and one roll were modelled (fig. 5). Both the roll and stock geometries closely reproduced the rolling mill used for the test and the sample described above.
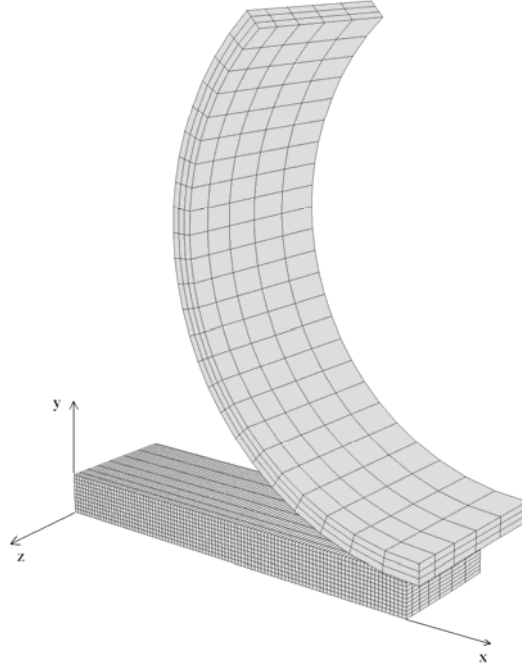
Figure 5 – Geometry and mesh in the initial undeformed position. The total number of nodes was 10,000.

The total number of nodes used for the model was 10,000. The chosen elements were suitable for coupled thermal-stress analysis. The computer used for the simulations consisted of a Pentium IV 3.2 GHz processor equipped with 1 GB RAM memory. Due to the high non-linearity of the problem, despite the relatively small number of nodes, the simulation took as long as 115 hours. This was the time needed for the whole stock to be completely rolled.

MATERIALS

The material behaviour of the slab was modelled using inverse hyperbolic sine functions (equation 4, 5, 6). These relationships model a viscoplastic behaviour linking the flow stress with temperature, strain and strain rate.

$$\sigma = \sigma_0 + \left(\sigma_{ss} - \sigma_0\right)\left[1 - e^{\left(-\frac{\varepsilon}{\varepsilon_r}\right)}\right]^m \qquad 4)$$

where

$$\sigma_0 = \frac{1}{A_1}\operatorname{arcsinh}\left[\left(\frac{Z}{A_2}\right)^{\frac{1}{n_0}}\right] \qquad 5)$$

$$\sigma_{ss} = \frac{1}{B_1}\operatorname{arcsinh}\left[\left(\frac{Z}{B_2}\right)^{\frac{1}{n_{ss}}}\right] \qquad 6)$$

7

$$Z = \overset{\bullet}{\varepsilon}\, e^{\left(\frac{Q_{def}}{R \cdot T}\right)}$$

7)

$$\varepsilon_r = C_1 + C_2 \cdot \sigma_{ss}^2$$

8)

The values of the parameters used in the above formulae (A_1, A_2, B_1, B_2, C_1, C_2, n_0, n_{ss}, m, Q_{def}) were fitted to stress/strain data obtained through hot plane strain compression tests [13]

The roll was modelled as steel working within its elastic response. Table 3 shows the physical constants used in the model for both roll and slab.

	Poisson's Ratio	Density [kg/m^3]	Specific Heat $[J/(kg \cdot K)]$	Conductivity $[W/(m \cdot K)]$	Coeff. of thermal expansion [K^{-1}]
roll	0.3	7833	615	50	1.2x0^{-5}
strip	0.3	2720	1050	203	2.31x10^{-5}

Table 3 – Material properties at room temperature for strip and roll.

In this numerical model, the fraction of plastic work per unit volume dissipated as heat was assumed to be 95% [14] and the heat generated by friction was equally distributed between the roll and the stock.

BOUNDARY CONDITIONS AND LOADS
The load history for this simulation consisted of three stages, each one characterized by different loads and boundary conditions.
Firstly, from the initial position of fig. 5, with the roll over the slab but not touching it, the roll moved down by 10% of the thickness of the sample, compressing the stock. In the meantime the nodes on the left side of the stock were constrained in the x direction to avoid the slab sliding away (stage 1). Subsequently the left-hand nodes of the stock were released. At this point the stock was compressed and clamped under the roll so that the combination of friction and pressure ensured that the stock did not move from this position. The roller moved down until the planned reduction ratio of 50 % was achieved (stage 2). Finally, the roll rotated at 11 rpm until the whole stock was rolled (stage 3).

TEMPERATURE AND HEAT TRANSFER COEFFICIENT
The heat transfer coefficient α between two surfaces in contact is defined by the equation:

$$\frac{dQ}{dt} = \alpha A \Delta T \,,$$

9)

where Q is the heat exchanged, A is the contact area and ΔT is the temperature difference between the two surfaces.
A constant *heat transfer coefficient* was used in the model and modified until the best match was found between the measured and computed temperature. The optimum constant

heat transfer coefficient was found to be 55 $kW/m^2 K$. Figure 6 shows a comparison between experimental and numerical values of temperature obtained using this value of the *heat transfer coefficient*.
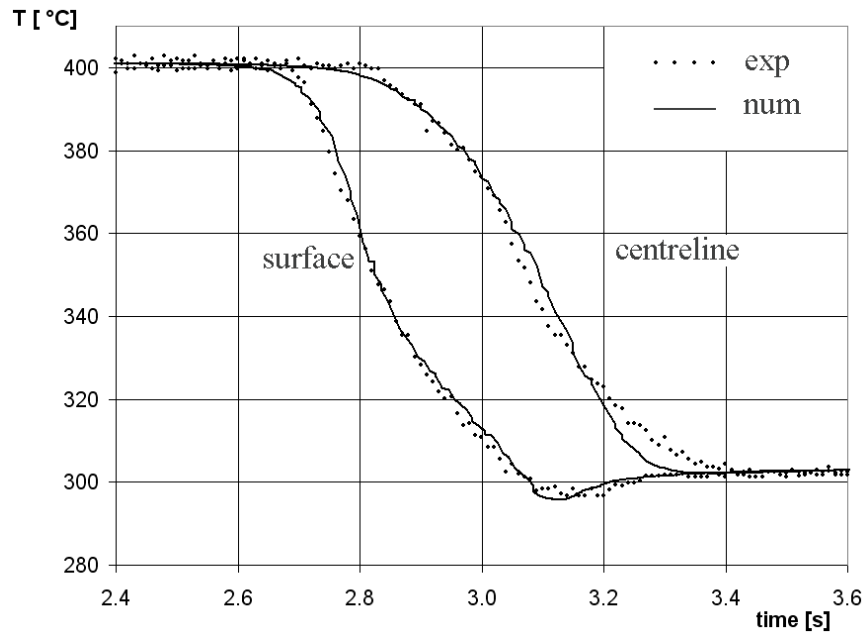
Figure 6 – Experimental (dots) and numerical (continuous lines) temperature profiles for the surface (left) and the centreline (right).

FRICTION AND DEFORMATION GRADIENT

The standard *Coulomb* friction model assumes that no relative motion occurs if the equivalent frictional stress τ_{eq} is less than the critical stress defined as

$$\tau_{cr} = \mu P, \qquad\qquad\qquad\qquad 10)$$

where *P* is the contact pressure and μ is the friction coefficient.
ABAQUS employs an extension of this classical isotropic *Coulomb* friction model that includes an additional limit on the allowable shear stress τ_{max} so that

$$\tau_{cr} = min(\mu P, \tau_{max}). \qquad\qquad\qquad\qquad 11)$$

Whenever the equivalent stress is at the critical stress or over, ABAQUS allows slip to occur between the surfaces.

The computed values of the components of the deformation gradient are highly dependent on the value of μ used in the model. This can be seen by changing the value of the friction coefficient used in the model: the slope of the vertical lines composing the mesh changes with the friction coefficient (fig. 7) and the deformation gradient tensor changes accordingly (in particular its *xy* component) . Hence the friction coefficient can be modified in order to match the shape of the deformed mesh with the deformed grid.

The best match between the experimental and numerical values of the deformation gradient tensor was found with a friction coefficient of 0.6 (fig. 7, bottom). This value is very close to the one expected in case of a sticking friction condition (μ=0.577).

9

friction coefficient 0.3

friction coefficient 0.4

friction coefficient 0.5

friction coefficient 0.6
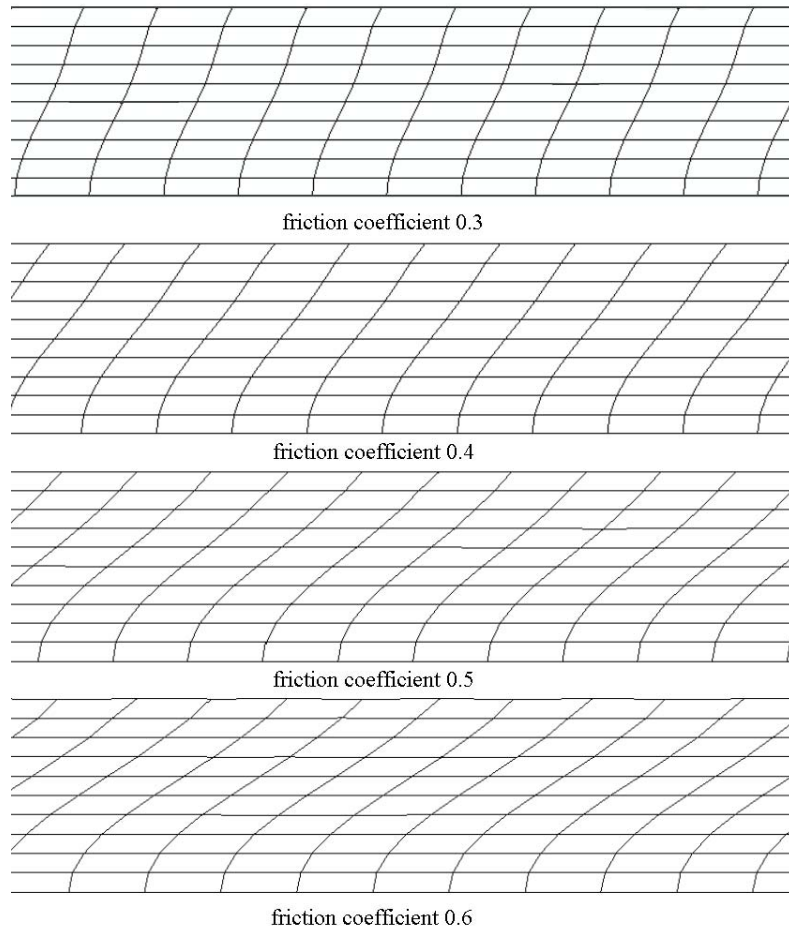
Figure 7 – Mesh variation on half of the slab thickness relative to different friction coefficients.

Figure 8 shows a comparison between the numerical and experimental deformation gradients over a length of about 14 *mm* along the insert for three different rows of element across the thickness (surface, quarter, centre).
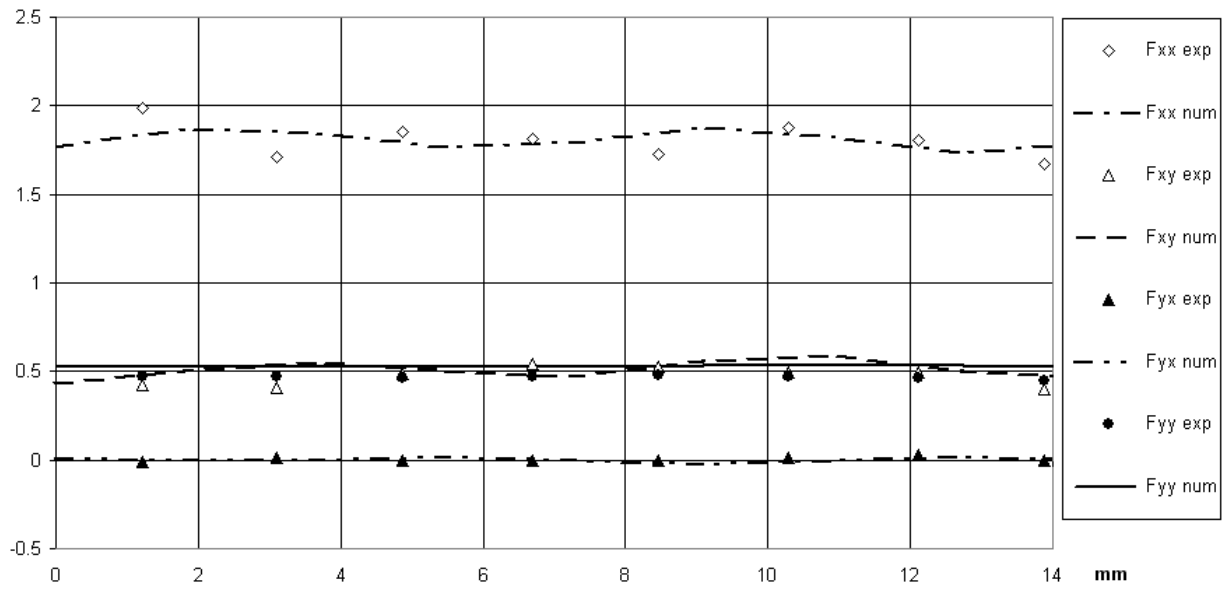
Figure 8a – Components of the deformation gradient tensor after exit from the mill for the top row of elements in an area of 14 *mm* in the middle of the slab. The reference frame is as in fig. 5.
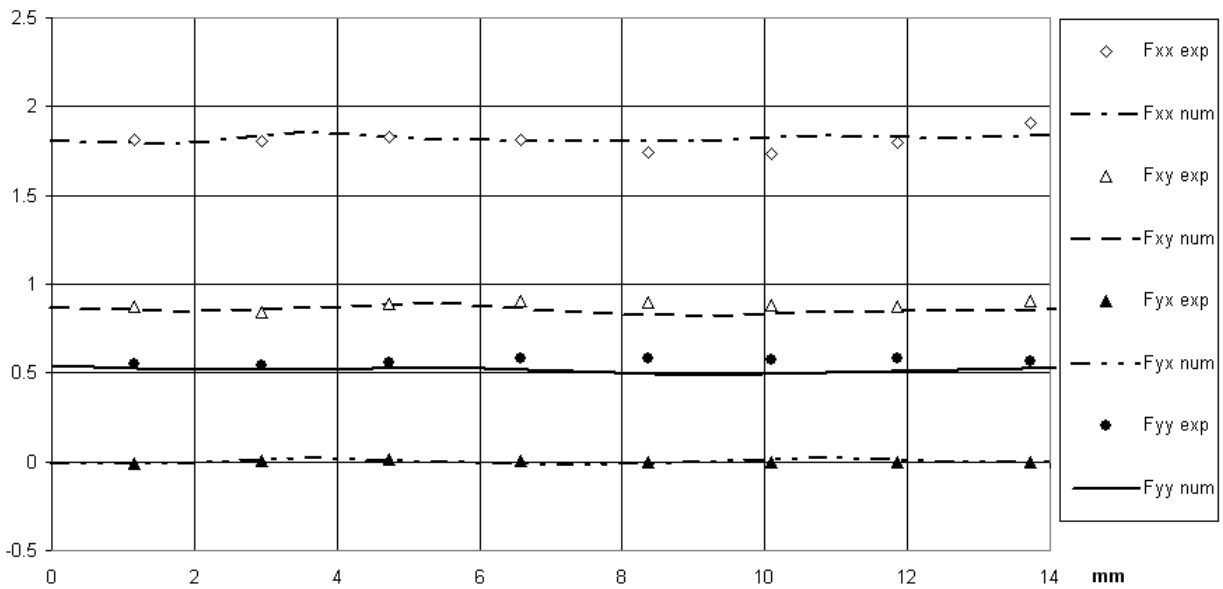
Figure 8b – Components of the deformation gradient tensor for a row of elements adjacent to the quarter-line of the insert. The reference frame is as in fig. 5.
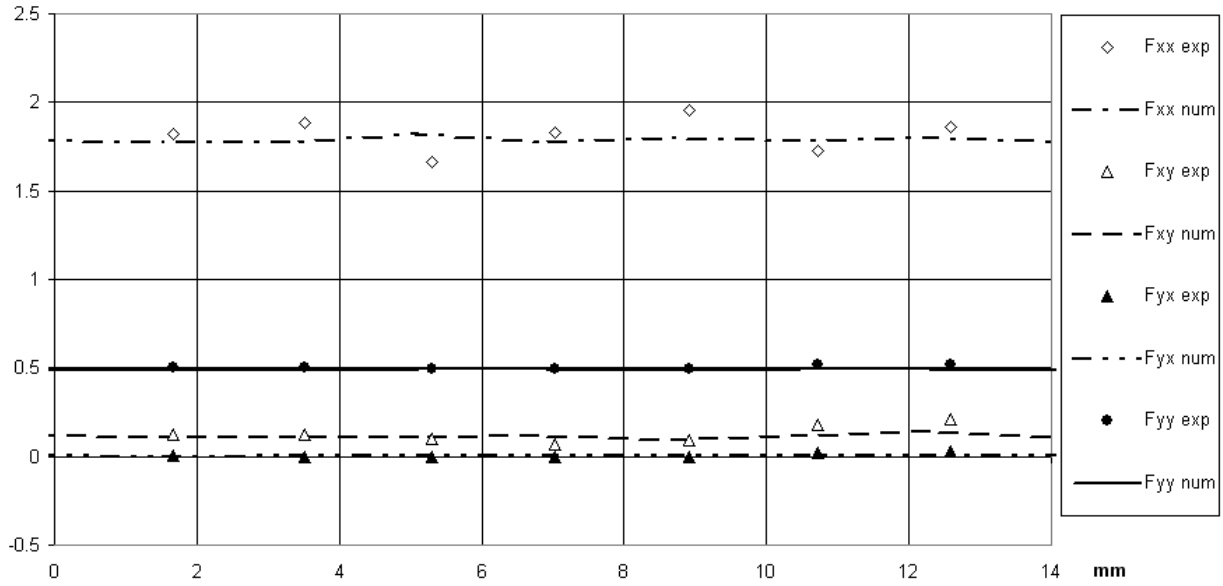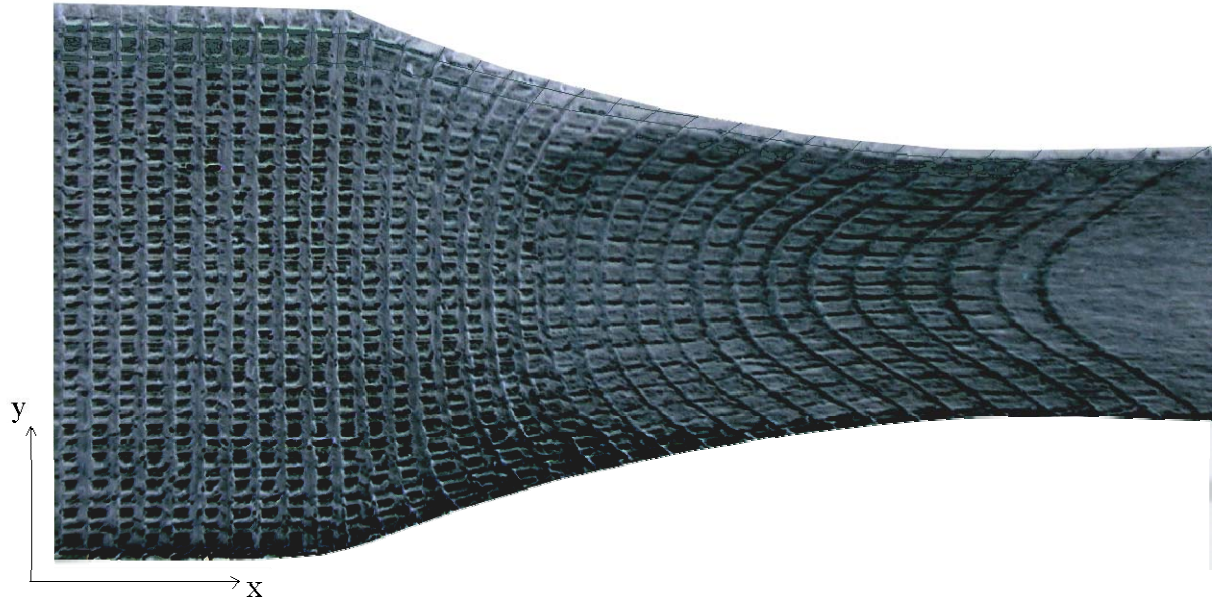
Figure 8c – Components of the deformation gradient tensor for a row of elements adjacent to the centre-line of the insert. The reference frame is as in fig. 5.

The width of the sample after rolling was measured resulting in a maximum spread of around 20% of the initial width: this result was accurately predicted by the model.

The comparison between numerical and experimental data shown in figure 8 is good, particularly so after considering the potential errors associated with the engraving method. Another source of inaccuracy in the measurement of the deformation gradient is due to the fact that the initial distance between two horizontal lines in the undeformed insert could not be *exactly 1 mm* in the first place. In fact, when the experimental deformation gradient is calculated by analyzing the picture, a constant pitch of *1 mm* is automatically assumed by the MATLAB script. If this distance was more than *1 mm* from the start, the final measurement of the strain along *y* would be less than the real one. The same applies to the F_{XY} component if the vertical lines are not exactly perpendicular to the horizontal lines in the first place.

TRANSITION STATE IN THE MILL

The roll gap area was also studied by analysing a picture obtained by stopping the rolls after they had rolled half of the length of the specimen. The top row of the grid was considered in figure 9 and the deformation gradient calculated for this row. The components of the deformation gradient for this row were then compared to the computed values (fig. 10).

Figure 9 – Deformed grid in the roll gap area, obtained by stopping the rolls. The deformation gradient was calculated for the top row of squares along the arc of contact.
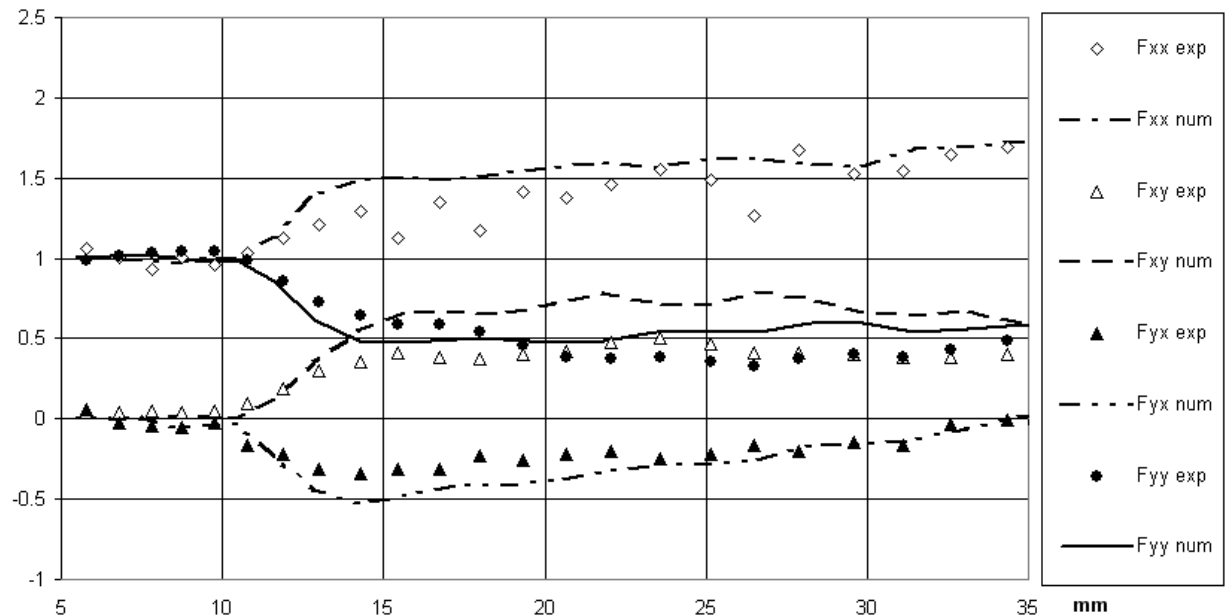
Figure 10 – Components of the deformation gradient in the roll gap area for the last row of elements close to the surface.

There is a very good qualitative agreement between these sets of data, and the quantitative comparison is very encouraging when considering the potential errors associated with the

engraving technique. Since this is the region of the deformation whose behaviour is affected most by the details of frictional load transfer at the interface, the comparisons of figure 10 are strong evidence for the effectiveness of using a constant value of the coefficient of friction for modelling such processes as these. The discrepancy between experimental and numerical data in this area can be explained by the large out-of-plane displacement observed on the partially rolled insert which also caused detachment between insert and work-piece. In fact, the gridded surface of the partially rolled insert was not as flat as the completely rolled insert, meaning that a portion of the deformation has developed in the transverse direction during rolling.

Discussion

This work has shown a way to measure the deformation gradient in a 50% reduction rolling pass. It is first important to stress that, despite the high reduction ratio, the grid was still visible after the test and no detachment was observed between the insert and the rest of the sample. This is an advantage compared to the embedded pin technique where detachment was observed between pin and sample [12]. The deformation gradients were calculated and an accuracy analysis was carried out to evaluate the error associated with the grid technique. The grid technique proved to be reliable for an experimental evaluation of the deformation gradient but various sources of error were found in the procedure itself mostly due to the width of the engraved lines and the manual nature of the procedure. However, the need for thinner grid-lines must take into account the necessity for a strong grid that would survive large deformations at high temperatures. Other automated engraving techniques, such as laser engraving and photo-etching, are being considered in order to improve the accuracy of the grid.

The high friction coefficient used in the numerical model was most probably related to a sticking condition between rolls and stock. Other experiments in the literature involving the same material but various rolling conditions produced a range of different friction coefficients, suggesting that finite element models have to be tailored to the actual rolling conditions. This is very important when the deformation gradients are extracted to be used as an input in texture prediction studies: this work shows that the use of a gridded insert is an accurate way to find the correct friction coefficient for the numerical code according to the rolling conditions and the material. Most importantly, the grid technique provided a true measurement of the deformation gradients through the thickness of the slab. This cannot be obtained with accuracy using other experimental techniques such as the embedded pin technique. An accurate prediction of the through-thickness deformation gradients means that the components of the deformation gradient tensor can be used in texture prediction programs with a high degree of confidence.

This is of major importance as far as texture is concerned since discrepancies between predicted and measured textures can therefore be attributed to the texture model itself and not to the input data.

Tuning the heat transfer coefficient was necessary to match experimental and numerical temperature profiles, the final results showing a very good match between predicted and measured temperatures. The numerical model built with a constant heat transfer coefficient provided similar results to the one with varying heat transfer coefficient. This proved that a constant heat transfer coefficient can be used in the finite element model without affecting the accuracy, resulting in a reduced computing time.

The finite element model in this work was more developed than in previous studies [5][8] where experiments were attempted to validate the numerical results. However, the high number of nodes and the non-linearity of the model made the simulation very time demanding with a running time of several hours.

Conclusions

In this research investigation, the use of an insert with an engraved grid was demonstrated as a viable method for obtaining deformation data that result from hot rolling of aluminium alloys. Any potential separation of the insert from the rest of the stock was eliminated by pinning the ends of the insert. This ensured that no gap occurred between insert and stock, which is an important condition for the accuracy of the technique.

This experimental method provided a powerful tool to validate finite element models of the rolling process. Numerical models were built and the comparison with the experimental data suggested that tuning the heat transfer and the friction coefficients between the stock and the rolls is necessary to create a reliable finite element model. Measurements of the thermal history obtained from embedded thermocouples were used to tune the heat transfer coefficients, while deformation gradient measurements obtained from the engraved grid were used to tune the friction coefficient.

Given the importance of measuring the deformation gradients for the forming processes, a rigorous method was developed to calculate its components automatically from a picture of the deformed grid area. Using this software, the deformation gradients were calculated in different areas of the rolled insert and compared with the numerical results. The agreement between experimental values of the components of the deformation gradient tensor and those derived from the tuned finite element model is qualitatively good for the roll-gap area, and quantitatively good for the output area. Improved quantitative agreement will very probably result from the use of grids created by more controlled, automated processes. Comparison of the deformation gradients measured in the roll-gap area with the ones predicted by the model proved that a single constant friction coefficient can be used in the model without loss of accuracy.

References

1   Kocks, U.F. et al., (eds) (1998). *Texture and Anisotropy.* Cambridge: Cambridge University Press
2   Basar, Y., Weichert, D., (eds) (2000) *Nonlinear continuum mechanics of solids* . Springer.
3. Wells, M.A., Lloyd, D.J., Samarasekara, I.V., Brimacombe J.K., Hawbolt, E.B., (1998). *Metallurgical And Materials Transactions B*, 29b, 709-719
4. Puchi, E.S., Beynon, J., Sellars, C.M., (1988). Proc. Int. Conf Of 'Physical Metallurgy Of Thermomechanical Processing Of Steels And Other Materials', *Thermec* 88, (Ed. I. Tamura), 572-579. Tokyo, Iron and Steel Institute of Japan
5. Timothy S. P., Yiu, H.L., Fine J. M., Ricks R.A., (1991). *Materials Science and Technology*, 7, 255-261
6. Lenard, J.G., Pietrzyk, M., Cser, L., (1999). 'Mathematical Simulation of the Properties of Hot Rolled Products'.Oxford: Elsevier.
7. 'Modelling of Metal Forming Processes 3', 13-15 December 1999, Church House Conference Centre, London, UK. IOM Comunications.
8. Beynon, J.H., Higginson, R.L., Pinna, C., (2000). 'Rolling experiments, texture measurements and computer-based predictions: closing the loop', Proceedings of the Conference Of Metallurgists, *Thermomechanical Processing of Steel*, Ottawa, Canada, August 2000, p. 121.
9. Wells, M.A., Maijer, D.M., Jupp, S. Lockhart G., Van Der Winder M.R., (2003). *Materials Science And Technology*, 19, 467-475
10. Li, E.B., Tieu, A.K., Yuen, W.Y.D., (2003). 'Application of digital image correlation technique to dynamic measurement of the velocity field in the deformation zone in cold rolling.' *Optics and Lasers in Engineering*, 39 479–488
11. Colonna, L., Dimitriou, R., Pinna C., Zhu, Q., (2003). 'Measurement of local strain heterogeneity in AA5182 after hot rolling deformation.' *Aluminium*, October, 393-397
12. Das, S., Palmiere, E., Howard, I.C., (2001). 'Effect of friction on deformation during rolling as revealed by embedded pin technique.' *Material Science and Technology*, Vol. 17, 865-873
13. Shi, H., Sellars, A.J., Shahani, R., Bolingbrode, R., (1997). 'Constitutive equations for high temperature flow stress aluminum alloys.' *Material Science and Technology*, March, Vol. 13, 210-216
14. Mielnik, E. M., *Metalworking science and engineering*, McGraw-Hill